Maneuvering Target Tracking with High-Order Correlated Noise – A Multirate Kalman Filtering Approach

DAH-CHUNG CHANG
N100, Computer and Communications Research Laboratories, Industrial Technology Research Institute, Chutung, Hsinchu, Taiwan 310, R.O.C.

WEN-RONG WU
Department of Communication Engineering, National Chiao Tung University, Hsinchu, Taiwan 300, R.O.C.
E-mail: wrwu@cc.nctu.edu.tw

Abstract. A multirate Kalman filtering algorithm for target tracking with high-order correlated noise is proposed. The measurement signal is first split into subbands using a filter bank. Then, the correlated noise in each subband is modeled using a first-order AR process and the AR parameters are identified online. Finally, a multirate Kalman reconstruction filter is used to obtain the state estimate. This method can be directly incorporated into the IMM algorithm, resulting in an effective tracking scheme. Simulations show that the new multirate processing scheme can significantly improve tracking performance.

Keywords: multirate Kalman filtering algorithm, filter banks, target tracking, correlated noise, IMM.

1. Introduction

The Kalman filter has been widely used in the radar target tracking problem. In that application, the measurement noise is usually assumed to be zero-mean white Gaussian. However, some researchers [1, 9] have reported that when the sampling rate of a radar system is high, the measurement noise is correlated. A common method to deal with this problem is to model the correlated noise by an AR process and include it in the state-space model. There are two ways of constructing the state-space model. One is the state augmentation method which explicitly includes the correlated noise in the state vector. This will result in the increase of the state dimension. The other is the decorrelation method which decorrelates the measurements using a filtering scheme. This approach changes the measurement equation, while the state dimension remains the same. In addition to the increase of the computational complexity, the state augmentation method can be ill-conditioned. Thus, the measurement decorrelation method is preferable in practice [1, 2, 6, 9].

While the measurement decorrelation method can solve the correlated noise problem, the only problem that remains is how to find the AR parameters. Many researchers assume that those parameters are known in advance. This may not be proper in real-world applications since the noise characteristics are not always known and, more importantly, they can be time-varying. In [1], we proposed an online parameter estimation method for a first-order AR-correlated noise. Simulation results showed that the algorithm in [1] can achieve almost the same tracking performance as when the AR parameters are exactly known. However, practical colored noise may not be well-modeled by the first-order AR process. Thus, higher
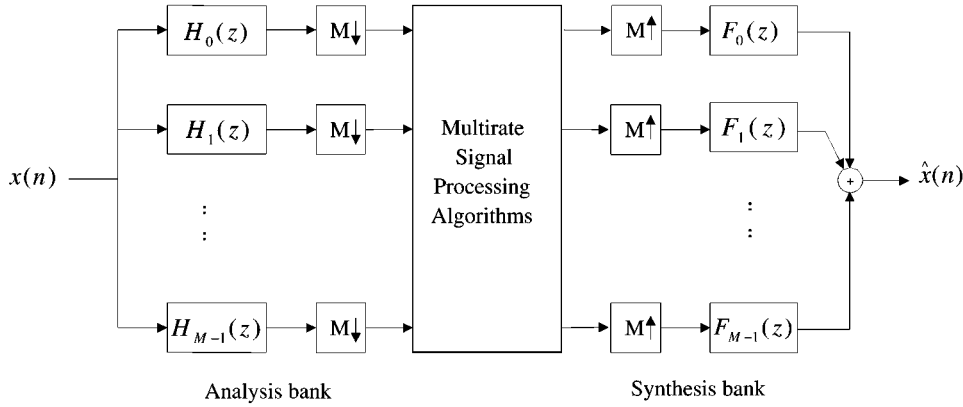
Figure 1. A typical multirate signal processing system.

order modeling is necessary. Unfortunately, it is found that a straightforward extension of the method in [1] is difficult. In this paper, we propose a new method to solve the problem.

The basic idea is that if a high-order correlated process can be split into subbands, then the shape of its power spectrum in each subband may become simple enough that a first-order AR model is sufficient. In other words, instead of a higher order AR noise model in fullband, we may consider a set of first-order AR models in subbands. Using this approach, we can then apply the method developed in [1] to estimate the AR parameters. Since the measurement signal is split into subbands, the state vector has to be represented in the subbands as well. This results in a multirate state-space representation of the target motion. A multirate Kalman filtering scheme, which estimates the state from its subband measurements, was proposed recently [13, 14]. We then use this algorithm to complete our tracking scheme. Note that the state transition matrix defined in the multirate Kalman filtering [13] is inherently singular. The decorrelation method in [1] requires the inverse of this state transition matrix. To overcome the problem, we use another decorrelation method which does not involve the matrix inverse.

This paper is organized as follows. Section 2 briefly reviews the multirate Kalman filtering algorithm [13] and the online identification algorithm for the first-order AR-correlated noise [1]. In Section 3, we describe target tracking with high-order AR-correlated noise using the multirate Kalman filtering scheme. Simulation results are demonstrated in Section 4 and conclusions are drawn in Section 5.

2. Multirate Kalman Filtering and Noise Identification

2.1. MULTIRATE KALMAN FILTERING

Multirate signal processing has attracted great attention recently. A typical system is shown in Figure 1. The input signal is first split into a set of subband signals using an M-channel analysis filter bank and M-fold decimators. Note that subband signals may be contaminated by noise. The processed signals are up-sampled by expanders and then processed by an M-channel synthesis filter bank to form the output signal. Many algorithms have been proposed [21, 24] to design the analysis/synthesis filters so that the output signal can perfectly reconstruct the input signal. However, most of them do not consider the subband noise. The work in [13] first considers the use of the Kalman filtering scheme for the signal reconstruction. The advantage of this approach is that the subband noise is explicitly taken into account and
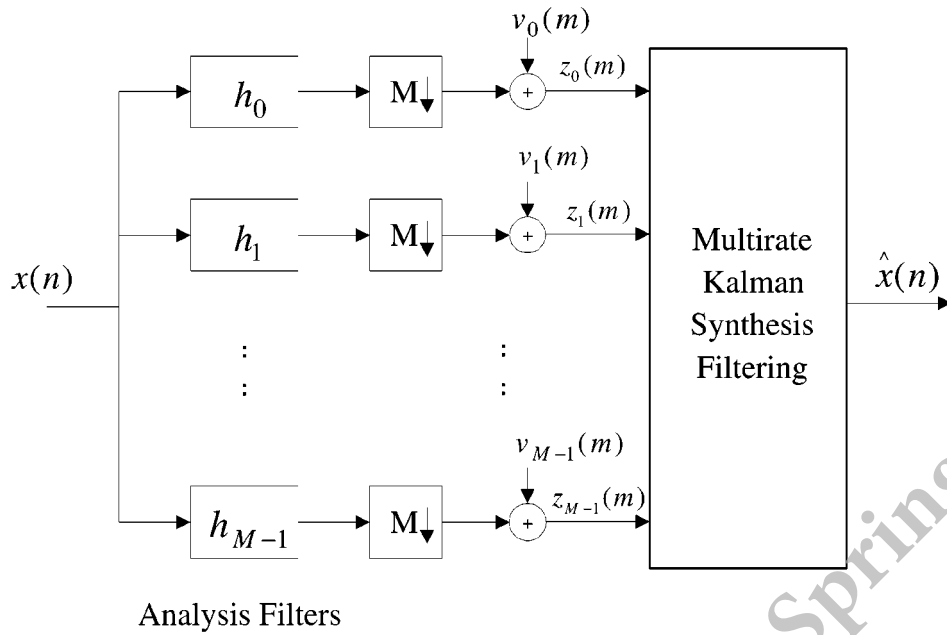
Figure 2. The multirate Kalman synthesis filter.

the result is optimal in the minimum mean square error sense. The structure of the multirate Kalman synthesis filter is depicted in Figure 2. Now, we briefly review the algorithm. Let the input signal $x(n)$ be modeled by a pth-order AR process,

$$x(n) = a_1 x(n-1) + a_2 x(n-2) + \cdots + a_p(n-p) + w(n), \tag{1}$$

where $w(n)$ is a zero-mean white Gaussian driving noise with variance $Q(n)$. The above equation can be rewritten as a state equation,

$$X_p(n) = A_p X_p(n-1) + G_p w(n), \tag{2}$$

$$X_p(n) = [x(n), x(n-1), \cdots, x(n-p+1)]^T, \tag{3}$$

$$A_p = \begin{bmatrix} a_1 & a_2 & \cdots & a_p \\ 1 & 0 & \cdots & 0 \\ 0 & \ddots & \cdots & 0 \\ 0 & 0 & 1 & 0 \end{bmatrix}_{p \times p}, \tag{4}$$

$$G_p = [1 0 \cdots 0]_{p \times 1}^T. \tag{5}$$

Since the measurements for the multirate Kalman synthesis filter are obtained from the outputs of the analysis filters, we increase the dimension of the input signal vector $X(n)$ to the filter length L (usually $L > p$), i.e.,

$$X(n) = [x(n), x(n-1), \cdots, x(n-L+1)]^T. \tag{6}$$

Then, the state equation becomes

$$X(n) = A X(n-1) + G w(n). \tag{7}$$

The matrix A and G (of dimensions $L \times L$ and $L \times 1$) can be easily derived from A_p and G_p. As we can see from Figure 2, the subband signal is M-fold down-sampled. Let the time index after down-sampling be m where $n = Mm + l, l = 0, 1, \cdots, M - 1$. Also, let the analysis filter response, the subband measurement, and the subband noise for the i-th band be $h_i(.)$, $z_i(m)$, and $v_i(m)$, respectively. Then, we can write the measurement equation as

$$Z(m) = HX(m) + V(m), \tag{8}$$

$$Z(m) = [z_0(m)z_1(m) \cdots z_{M-1}(m)]^T, \tag{9}$$

$$V(m) = [v_0(m)v_1(m) \cdots v_{M-1}(m)]^T, \tag{10}$$

$$H = \begin{bmatrix} h_0(0) & h_0(1) & \cdots & h_0(L-1) \\ h_1(0) & h_1(1) & \cdots & h_1(L-1) \\ \vdots & \vdots & \vdots & \vdots \\ h_{M-1}(0) & h_{M-1}(1) & \cdots & h_{M-1}(L-1) \end{bmatrix}. \tag{11}$$

Note that the state $X(k)$ in (7) and the measurement signal $Z(k)$ in (8) have different rates, i.e., $\{X(k), k = 0, 1, 2, \cdots\}$ and $\{Z(k), k = 0, M, 2M, \cdots\}$. Using the recursive relation in (7), we can obtain

$$X(n + M) = A^M X(n) + G_M W(n + M), \tag{12}$$

$$G_M = [G \ AG \ A^2 G \cdots A^{M-1} G], \tag{13}$$

$$W(n + M) = [w(n + M)w(n + M - 1) \cdots w(n + 1)]^T. \tag{14}$$

Then, Equation (12) can be written as

$$X(m + 1) = A^M X(m) + G_M W(m + 1). \tag{15}$$

From the above results, we have a multirate state-space model describing the input signal and the measurement.

$$X(m + 1) = A^M X(m) + G_M W(m + 1), \tag{16}$$

$$Z(m) = HX(m) + V(m). \tag{17}$$

Thus, the standard Kalman filtering scheme can be applied to obtain the state estimate. Since the state equation is represented by the time index m and $n = Mm$, the Kalman filter outputs a state estimate every M samples. To achieve better reconstruction results, we can take the results after some time delay.

$$\begin{bmatrix} \hat{x}(n - l) \\ \hat{x}(n - l - 1) \\ \vdots \\ \hat{x}(n - l - M + 1) \end{bmatrix} = \begin{bmatrix} \mathbf{0}_{M \times l} & \mathbf{I}_{M \times M} & \mathbf{0}_{M \times (L-l-M)} \end{bmatrix} \hat{X}(m), \tag{18}$$

where l is the delay ranging from 0 to $L - M$, $\mathbf{0}$ is a zero matrix, and $\mathbf{I}$ is an identity matrix. As l increases, the performance of reconstruction is improved. The best reconstruction result is obtained by choosing $l = L - M$.

2.2. IDENTIFICATION OF FIRST-ORDER AR-CORRELATED NOISE

The work in [1] uses the measurement decorrelation method. Consider a one-dimensional tracking problem.

$$X(n + 1) = \phi X(n) + Gw(n + 1) \tag{19}$$

$$z(n) = HX(n) + v(n), \tag{20}$$

where $X(n)$ is the state vector, ϕ is the state transition matrix, $z(n)$ is the measurement, and $w(n)$ and $v(n)$ are the state and the measurement noises, respectively. Rogers [2] modeled the correlated noise as a first-order AR process, which can be described by

$$v(n) = \alpha v(n - 1) + \eta(n), \tag{21}$$

where $\eta(n)$ is zero-mean white Gaussian noise with variance σ_η^2. Define a new measurement $\bar{z}(n)$ as

$$
\begin{aligned}
\bar{z}(n) &\stackrel{\triangle}{=} z(n) - \alpha z(n - 1) \\
&= \bar{H}x(n) + \bar{\eta}(n),
\end{aligned}
\tag{22}
$$

where

$$\bar{H} = H(I - \alpha\phi^{-1}), \tag{23}$$
$$\bar{\eta}(n) = \alpha\phi^{-1}HGw(n + 1) + \eta(n) \tag{24}$$
$$\approx \eta(n). \tag{25}$$

In (24), the first term of the right-hand side is usually small and can be neglected. Thus, $\bar{\eta}(n)$ can be treated as a white process. Using $\bar{z}(n)$ as the measurement, the standard Kalman filter can be applied. To describe the algorithm in [1], we assume that the measurement is the target's position. Let $X(n) = [x(n)\ s(n)\ a(n)]^T$, where $x(n)$, $s(n)$, and $a(n)$ are target position, velocity, and acceleration, respectively. We then have the measurement equation

$$z(n) = [1\ 0\ 0]X(n) + v(n). \tag{26}$$

Since measurements contain the state variable $x(n)$, the direct estimation of the AR parameters is difficult. Note that $x(n)$ corresponds to a lowpass signal. Thus, we can use a highpass filter to remove it. The specially designed highpass filter in [1] has the z-transform as follows:

$$F(z) = \frac{(1 - z^{-1})^2}{(1 - \rho z^{-1})^2}, \tag{27}$$

where $\rho < 1$. It was shown in [1] that for the constant velocity target, the state variable can be completely removed using this filtering operation. Let the input and the output of the filter $F(z)$ be $z(n)$ and $u(n)$, respectively. Denote the autocorrelation function of $u(n)$ as $r(.)$. Then, the parameters α and σ_η^2 can be found as follows:

$$\alpha = \frac{-(\xi_3 + \xi_2) - \sqrt{(\xi_3 + \xi_2)^2 - 4\xi_3(\xi_3 + \xi_2 + \xi_1)}}{2\xi_3} \tag{28}$$

and

$$\sigma_\eta^2 = -\frac{[-2\rho^3\alpha^2 + (1-\rho^4)\alpha + 2\rho]r(0) + [(\rho^2+\rho^4)\alpha^2 + (2\rho^3-2\rho)\alpha - (\rho^2+1)]r(1)}{(1+\rho^2)\alpha + (2\rho-4)} . \quad (29)$$

where

$$\alpha_b = \frac{r(1)}{r(0)} \quad (30)$$

$$\xi_3 = (\rho+1)^3 \quad (31)$$

$$\xi_2 = (-2\rho^2 - 10\rho - 4) + (-6\rho - 2)\alpha_b \quad (32)$$

$$\xi_1 = (-\rho^3 - 3\rho^2 + 5\rho + 7) + (8\rho + 8)\alpha_b \quad (33)$$

$$\xi_0 = (2\rho^2 + 2\rho - 4) + (-2\rho - 6)\alpha_b . \quad (34)$$

Substituting $r(1)$ and $r(0)$ with their estimates $\hat{r}(1)$ and $\hat{r}(0)$, we can obtain $\hat{\alpha}(n)$ and $\hat{\sigma}_\eta^2(n)$. The estimates $\hat{r}(1)$ and $\hat{r}(0)$ at time n can be calculated as

$$\hat{r}_n(0) = \beta\hat{r}_{n-1}(0) + (1-\beta)u^2(n) \quad (35)$$

$$\hat{r}_n(1) = \beta\hat{r}_{n-1}(1) + (1-\beta)u(n)u(n-1) , \quad (36)$$

where $0 < \beta < 1$ is a forgetting factor.

3. Multirate Kalman Tracking Algorithm for High-Order Correlated Noise

3.1. NOISE IDENTIFICATION IN SUBBAND

Although the AR identification scheme described in Section 2 is effective, it can only be applied to the first-order AR process. Practical correlated noise may not be well modeled by the first-order AR process. Here, we consider extending its application to high-order AR-correlated noise. However, we find that it is difficult to extend the similar method as described in Section 2 to identify high-order AR noise. Here, we propose another approach. Our observation is that the parameter estimation problem may be viewed as a spectrum fitting problem. The power spectrum of a first-order AR model is too simple to fit a general complicated spectrum. However, if we can split the noise signal into subbands, then the shape of its power spectrum in each subband will become much simpler. In this case, the first-order AR modeling may be sufficient. To achieve this, the measurement signal has to be decomposed into subbands. Let the measurement equation be the same as that in (26), i.e.,

$$z(n) = x(n) + v(n) . \quad (37)$$

The measurement signal is first split into a set of subband signals $z_i(m)$ by an M-channel analysis filter bank and M-fold decimators. The subband measurement signals can be expressed as

$$z_i(m) = x_i(m) + v_i(m) , \quad (38)$$

where $x_i(m)$ is the i-th subband signal of $x(n)$ and $v_i(m)$ is that of $v(n)$. Thus, a multirate Kalman filtering structure as depicted in Figure 2 can be applied to obtain the state estimate. It is worth noting that the formulation here is not exactly identical to that in Figure 2. The noise $v_i(m)$'s in Figure 2 are added in the subbands, while $v_i(m)$'s in (38) are added in the fullband.

As a conseqeunce, the noise $v_i(m)$'s in Figure 2 are uncorrelated, while $v_i(m)$'s in (38) are correlated. Fortunately, the correlations are usually small and their effect can be neglected.

Now, let us see what the target motion will become in the subband domain. From (11), we can see that

$$x_i(m) = \sum_{k=0}^{L-1} h_i(k)x(mM - k) \,. \tag{39}$$

Equation (39) can be interpreted as $x_i(m)$ is a linear combination of the functions $x(mM)$, $x(mM - 1), \ldots,$ and $x(mM - L + 1)$. The following observation is useful in the later discussion.

Observation: The linear combination of N-th order polynomials is also an N-order polynomial.

Thus, if the target has a constant velocity, then $x(n - i), i = 0, 1, \ldots,$ is a linear function of time and so is $x_i(m)$. If the target has a constant acceleration, then $x(n - i), i = 0, 1, \ldots,$ is a quadratic function of time and so is $x_i(m)$. We can then conclude that the target motion in each subband has similar characteristics as that in fullband. The velocity/acceleration in each subband is different from that in the fullband only by a factor. As a result, the noise extraction method in [1] can be directly applied in subband. We now conduct a simulation to verify this result. We use a 5-band cosine-modulated analysis bank and the prototype filter has 20 taps. The frequency responses of the filter bank are plotted in Figure 3. We consider the same target track used in [1] and [7], except that the sampling period here is 0.01. The original target track and the subband tracks are shown in Figure 4 in which the x-axis is the sample numbers and the y-axis is the target position in dB unit. It is clear that the target tracks in the subbands are very similar to the original track and there exists a nearly constant difference. This is consistent with our assertion above.

3.2. THE NEW TRACKING ALGORITHM

Assume that the measurement is the target position which is corrupted by correlated noise. The measurement signal is first passed through an analysis filter bank and then the state estimate is performed by the multirate Kalman synthesis filter. As we described, the state dimension has to be increased to L, the length of the analysis filter. Define the state vector as

$$
\begin{aligned}
X(n) = & [x(n), x(n - 1), \cdots x(n - L + 1), s(n), s(n - 1), \cdots \\
& s(n - L + 1), a(n), a(n - 1), \cdots, a(n - L + 1)]^T \,,
\end{aligned} \tag{40}
$$

where $x(n), s(n),$ and $a(n)$ are the target position, velocity, and acceleration, respectively. The target state equation can be written as

$$X(n + 1) = FX(n) + Gw(n + 1) \,, \tag{41}$$

where $w(n)$ is the target acceleration increment assumed to be a white Gaussian process [15] and F is the $3L \times 3L$ transition matrix. For example, if $L = 3$, then

$$
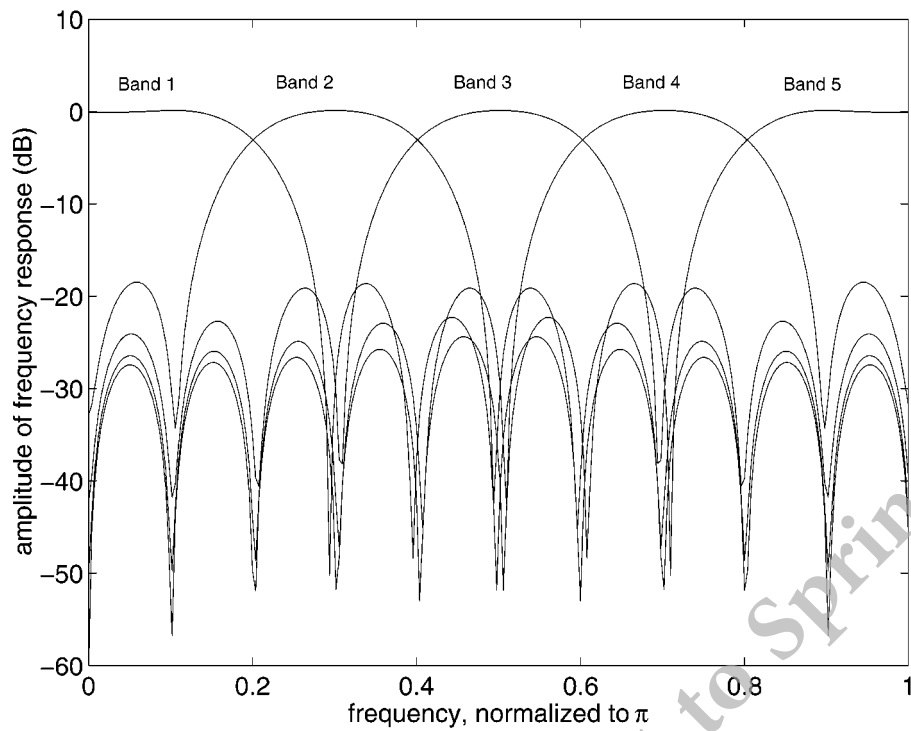F = \begin{bmatrix} F_{11} & F_{12} & F_{13} \\ F_{21} & F_{22} & F_{23} \\ F_{31} & F_{32} & F_{33} \end{bmatrix} \,, \tag{42}
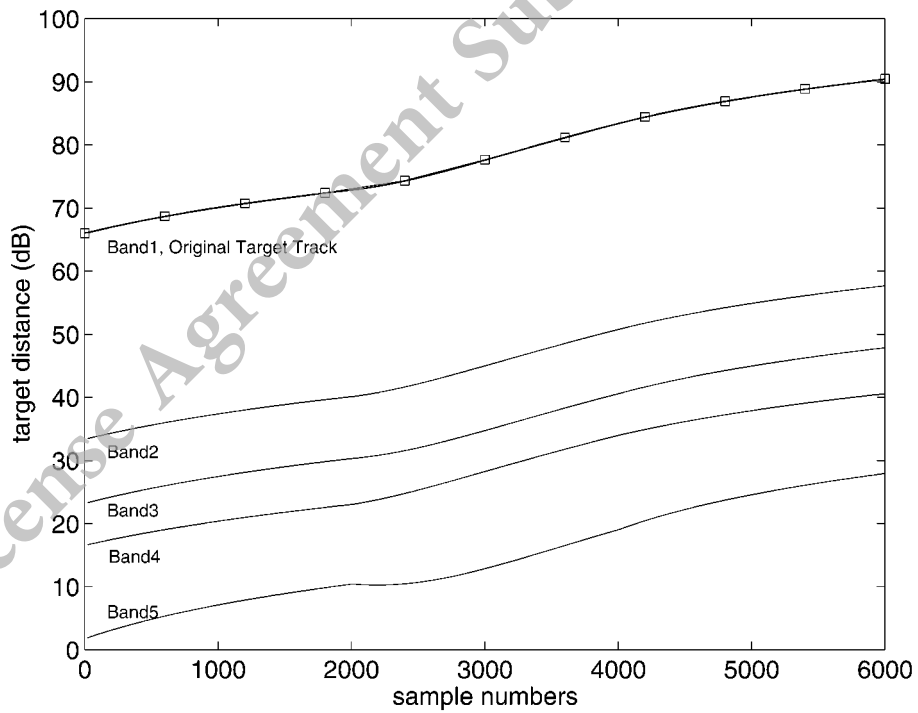$$

Figure 3. The amplitude response of the analysis bank.

Figure 4. The original and subband target tracks.

where

$$F_{11} = F_{22} = F_{33} = \begin{bmatrix} 1 & 0 & 0 \\ 1 & 0 & 0 \\ 0 & 1 & 0 \end{bmatrix},$$

$$F_{12} = F_{23} = \begin{bmatrix} T & 0 & 0 \\ 0 & 0 & 0 \\ 0 & 0 & 0 \end{bmatrix}, F_{13} = \begin{bmatrix} T^2/2 & 0 & 0 \\ 0 & 0 & 0 \\ 0 & 0 & 0 \end{bmatrix}, \tag{43}$$

$$F_{21} = F_{31} = F_{32} = \begin{bmatrix} 0 & 0 & 0 \\ 0 & 0 & 0 \\ 0 & 0 & 0 \end{bmatrix},$$

and T is the sampling period. The vector G is a $3L \times 1$ column vector, which is

$$G = [T^2/2 \ 0 \cdots 0 \ T \ 0 \cdots 0 \ 1 \ 0 \cdots 0]^T. \tag{44}$$

Replacing the time index n by its decimated version m, we can write the multirate state equation as

$$X(m+1) = F^M X(m) + G_M W(m+1), \tag{45}$$

$$G_M = [G \ FG \cdots F^{M-1}G]. \tag{46}$$

Let the subband inputs to the multirate Kalman synthesis filter be $z_i(m)$, $i = 0, 1, \cdots, M-1$. Then, the multirate measurement equation is

$$Z(m) = HCX(m) + V(m), \tag{47}$$

$$Z(m) = [z_0(m)z_1(m) \cdots z_{M-1}(m)]^T, \tag{48}$$

$$H = \begin{bmatrix} h_0(0) & h_0(1) & \cdots & h_0(L-1) \\ h_1(0) & h_1(1) & \cdots & h_1(L-1) \\ \vdots & \vdots & \ddots & \vdots \\ h_{M-1}(0) & h_{M-1}(1) & \cdots & h_{M-1}(L-1) \end{bmatrix}, \tag{49}$$

$$C = [\mathbf{I}_{L \times L} \ \mathbf{0}_{L \times L} \ \mathbf{0}_{L \times L}], \tag{50}$$

where $V(m) = [v_0(m)v_1(m) \cdots v_{M-1}(m)]^T$ represents the correlated noise vector in the subband. Each $v_i(m)$ is modeled using a first-order AR process. Thus, $V(m)$ can be rewritten as the following equation.

$$V(m) = DV(m-1) + E(m), \tag{51}$$

$$D = \begin{bmatrix} \alpha_0 & 0 & \cdots & 0 \\ 0 & \alpha_1 & \cdots & 0 \\ \vdots & \vdots & \ddots & \vdots \\ 0 & 0 & \cdots & \alpha_{M-1} \end{bmatrix}, \tag{52}$$

$$E(m) = [\eta_0(m)\eta_1(m)\cdots\eta_{M-1}(m)]^T, \tag{53}$$

where α_i is the AR coefficient for the $(i+1)$th subband and $\eta_i(m)$ is a white Gaussian driving noise for the $(i+1)$th subband.

The measurement decorrelation method needs to compute the artificial measurement defined as

$$\begin{align}
\bar{Z}(m) &= Z(m) - DZ(m-1) \tag{54}\\
&= \bar{H}X(m) + \bar{E}(m), \tag{55}
\end{align}$$

where

$$\begin{align}
\bar{H} &= HC - DHC(F^M)^{-1} \tag{56}\\
\bar{E}(m) &= DHC(F^M)^{-1}G_M W(m) + V(m) - DV(m-1)\\
&\approx V(m) - DV(m-1)\\
&= E(m). \tag{57}
\end{align}$$

Unfortunately, the matrix F^M is a singular matrix and its inverse does not exist. The conventional decorrelation method cannot be used here. Therefore, we propose to use another decorrelation method. Let

$$\begin{align}
Z_b(m) &= Z(m+1) - DZ(m) \tag{58}\\
&= H_b X(m) + E_b(m+1), \tag{59}
\end{align}$$

where

$$\begin{align}
H_b &= HCF^M - DHC\\
E_b(m+1) &= HCG_M W(m+1) + V(m+1) - DV(m)\\
&\approx V(m+1) - DV(m)\\
&= E(m+1). \tag{60}
\end{align}$$

Although this decorrelation method can avoid the calculation of $(F^M)^{-1}$, it requires the measurement $Z(m+1)$. This will delay the tracking by one block samples (M to $2M-1$ samples). If the delay is not desirable, we may use (45) to output the predicted state. The other method is to use linear extrapolation to obtain an estimate of $X(m) - X(m-1)$ such that a measurement equation involving $\bar{Z}(m)$ can be used. We now describe this method in detail. Using the relation $\bar{Z}(m) = Z_b(m-1)$, we have

$$\begin{align}
\bar{Z}(m) &= Z_b(m-1) \tag{61}\\
&= H_b X(m-1) + E(m) \tag{62}\\
&= H_b X(m) - H_b[X(m) - X(m-1)] + E(m) \tag{63}\\
&\approx H_b X(m) - H_b F^M[\hat{X}(m-1) - \hat{X}(m-2)] + E(m). \tag{64}
\end{align}$$

When the target is nonmaneuvering, this extrapolation error is almost zero. When the target is maneuvering, there is some performance degradation using this approximation. From (64), we can see that to use H_b (instead of $\bar{H}$), a term $H_b[X(m) - X(m-1)]$ must be subtracted from $\bar{Z}(m)$. When the target has a constant velocity, this term is constant also. We can consider

it as a bias term. From the above derivation, we can have the new multirate Kalman filtering algorithm for decorrelating high-order AR-correlated noise. The state and measurement equations can be written as follows:

$$X(m + 1) = F^M X(m) + G_M W(m + 1),$$ (65)

$$\bar{Z}(m) = H_b X(m) - B(m) + E(m),$$ (66)

$$B(m) = H_b F^M [\hat{X}(m - 1) - \hat{X}(m - 2)],$$ (67)

where $\hat{X}(m - 1)$ and $\hat{X}(m - 2)$ can be obtained from the past state estimations using Kalman filtering. Note that both the prediction method and the method in (66) are suboptimal. As shown in the expression of (18), the multirate Kalman filter will output a state estimate every M samples and we have many ways to output data. The delay ranges from $l = 0$ to $l = L - M$ in (18). Note that for $l = 0$, there still exists a 0 to $M - 1$ sample delay. This is due to the multirate processing effect mentioned above. This delay can be reduced by choosing a small subband number. Depending on the applications, a certain degree of delay can be tolerable [16, 19].

In this paragraph, we discuss the computational complexity of the proposed algorithm. A Kalman filter requires $O(3ln^2)$ multiplications for each iteration where l and n are the measurement and state dimensions, respectively. Since the dimension of the multirate Kalman filter is greatly increased, the computational complexity should be much higher than that of the single rate Kalman filter. Fortunately, there are many zeros in the state transition matrix. Thus, the computational complexity can be effectively reduced. In general, we can say that the required computational complexity for the multirate Kalman filter is close to that of the single rate Kalman filter. Only the storage for the computed parameters will be higher. Of course, extra computations are necessary for the filter bank operations.

4. Simulations

We use a one-dimensional range tracker to demonstrate the effectiveness of the proposed algorithm. The IMM algorithm [20] is used as the tracking algorithm, which is implemented using a second-order model for the nonmaneuvering mode and two third-order models for the maneuvering mode; one has process noise and the other has no process noise. The target state equations corresponding to (41) are described below. For notational simplicity, only the case for $L = 1$ is shown.

1. Nonmaneuvering mode,

$$\begin{bmatrix} x(n + 1) \\ s(n + 1) \end{bmatrix} = \begin{bmatrix} 1 & T \\ 0 & 1 \end{bmatrix} \begin{bmatrix} x(n) \\ s(n) \end{bmatrix} + \begin{bmatrix} T \\ 1 \end{bmatrix} w(n + 1)$$ (68)

2. Maneuvering mode,

$$\begin{bmatrix} x(n + 1) \\ s(n + 1) \\ a(n + 1) \end{bmatrix} = \begin{bmatrix} 1 & T & \frac{1}{2}T^2 \\ 0 & 1 & T \\ 0 & 0 & 1 \end{bmatrix} \begin{bmatrix} x(n) \\ s(n) \\ a(n) \end{bmatrix} + \begin{bmatrix} \frac{1}{2}T^2 \\ T \\ 1 \end{bmatrix} w^m(n + 1)$$ (69)

where $w(n)$ and $w^m(n)$ are white noises. In the simulation, the sampling period is taken as 0.01 sec. The total tracking interval is 60 sec. In other words, there are 6,000 measurement samples. The maneuvering occurs from the 20th to the 40th sec with a constant acceleration of 40 m/sec^2 (about $4g$). The target track is the same as that shown in Figure 4.

The three IMM models are defined as follows:

Model 1: a constant velocity model for nonmaneuvering. The process noise variance is $E[w(n)w(n)] = 10^{-4}$ (m/sec^2)^2.

Model 2: a large acceleration model for maneuvering. The process noise variance is $E[w^m(n)$ $w^m(n)] = 40^2$ (m/sec^2)^2.

Model 3: a constant acceleration model for maneuvering. The process noise is zero, i.e., $w^m(n) = 0$.

The Markovian transition probability matrix of the three models is chosen as

$$[p_{ij}] = \begin{bmatrix} 0.99 & 0.01 & 0.00 \\ 0.33 & 0.34 & 0.33 \\ 0.00 & 0.01 & 0.99 \end{bmatrix}. \tag{70}$$

Here, we assume that the correlated noise is a third-order AR process described by

$$v(n) = 0.8v(n-1) - 0.7v(n-2) + 0.6v(n-3) + \eta(n), \tag{71}$$

where $\eta(n)$ is a zero-mean white Gaussian noise with variance 100^2 m^2. The power spectrum of the correlated noise has two peaks; one is around the zero frequency, the other around 0.5π. The amplitude of the power spectrum is plotted in Figure 5. A 5-band cosine-modulated analysis bank with the 20 taps prototype filter is used. The frequency responses of the filter bank are plotted in Figure 3. The simulation setup is the same as that in [1]. A total of 500 Monte Carlo runs are carried out and the averaged root mean square error (RMSE) is used as the performance criterion.

$$\text{RMSE}(n) = \sqrt{\frac{1}{N}\sum_{i=1}^{N}[x(n) - \hat{x}^i(n)]^2}, \quad n = 1, 2, \cdots, 6000; \quad N = 500, \tag{72}$$

where $\hat{x}^i(n)$ denotes the state estimate of the ith Monte Carlo simulation for the nth sample.

The two parameters used in the noise extraction process were chosen as $\rho = 0.095$ and $\beta = 0.995$. We used these two parameter values in each subband. The identification results (a single run) for the AR coefficients in the subbands are shown in Figure 6 and their corresponding driving noise variances are shown in Figure 7. As we can see, the estimated results for these two parameters do not experience significant varying during the maneuvering. However, variations at the beginning are large. This is due to the use of a large β. To speed up the convergence, we let β be time-variant. Starting with smaller values at the initial, β increases gradually. The following function is used for β.

$$\beta(m) = 0.995 - 0.5e^{-m/\lambda}, \tag{73}$$

where λ is a decay constant. Given a desired value at a desired time, λ can be easily calculated. For example, if we set $\beta(m_0)$=0.994, then
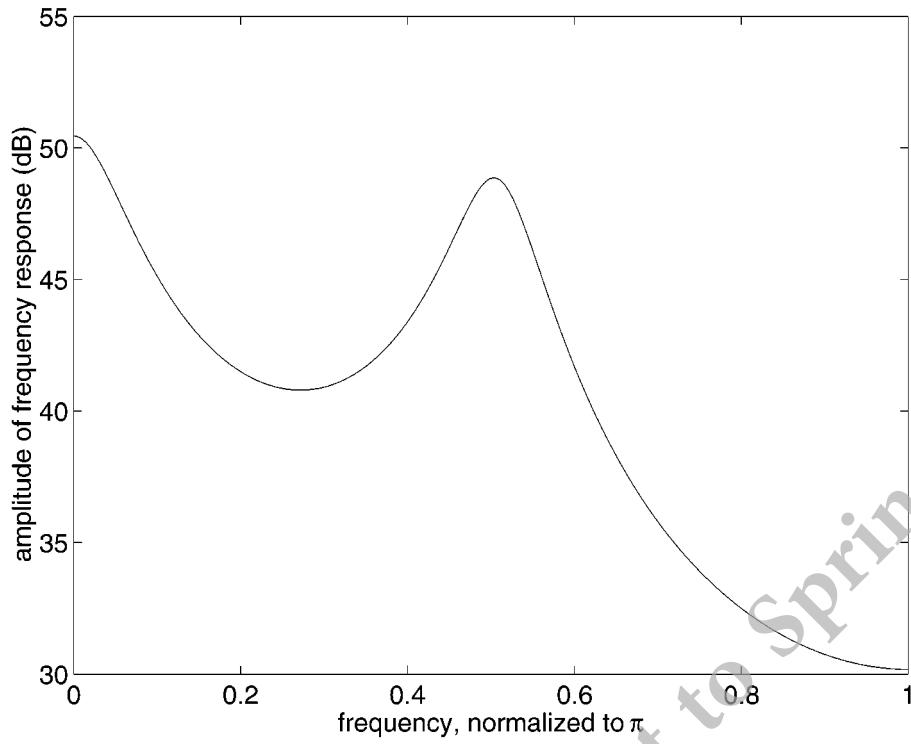
$$\lambda = m_0/log(0.5/0.001). \tag{74}$$

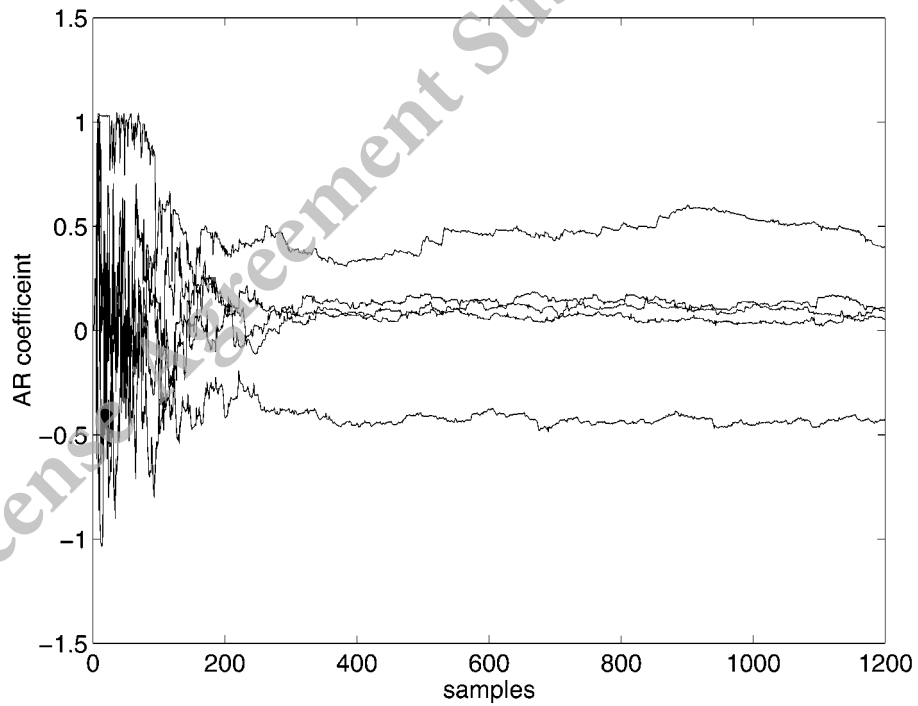*Figure 5.* The power spectrum of the three-order AR colored noise.

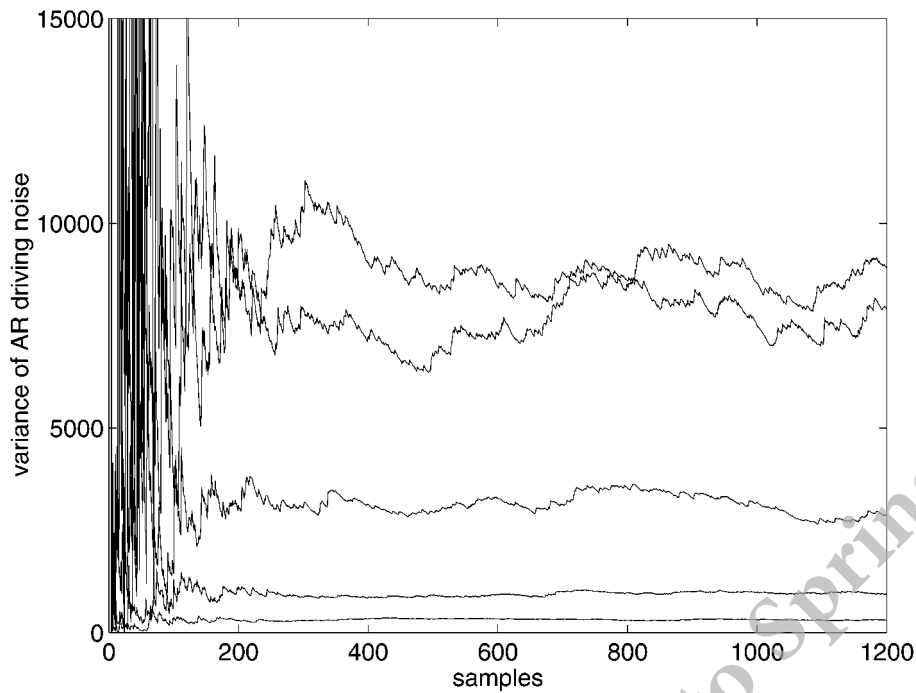*Figure 6.* The learning curves for the AR coefficients in subbands.

Figure 7. The learning curves for the variances of AR driving noise in subbands.

The parameter β will finally converge to 0.995 as m goes to infinity. Here, we set $m_0 = 400$ in the simulation.

Using the correlated noise given by (71), we compare the tracking performance of four algorithms. In the first one, we consider the conventional Kalman filtering algorithm in which there is no other processing for the correlated noise. In this case, the white noise assumption is violated and the Kalman filter is no longer the optimal filter. In the second one, we assume that the parameters of the third-order AR-correlated noise are exactly known. Then, we can directly apply the decorrelation method in (58). Using the expression in (19) and (20), the decorrelated measurement equation is

$$\bar{z}(n) = \bar{H}x(n - 3) + \eta(n) \tag{75}$$

$$\bar{H} = H\phi^3 - \alpha_1 H\phi^2 - \alpha_2 H\phi - \alpha_3 H , \tag{76}$$

where α_1, α_2, and α_3 are the three AR coefficients and $\eta(n)$ is the white Gaussian driving noise. In the third one, we use the proposed subband processing algorithm. Here, we consider the optimal result in which the output delay is set to 15 ($l = 15$) and (58) is used for decorrelation. Later, we will consider the case where $l = 0$ and (66) is used. In the fourth one, we apply the first-order AR-decorrelation algorithm proposed in [1] (although the noise is third-order AR-correlated noise). The tracking results for target position, velocity, and acceleration are shown in Figures 8–10. We can see that the proposed subband first-order AR-decorrelation process has the best performance. The performance of the exact third-order AR-decorrelation method is still inferior to the proposed one. This is due to the delay operations (smoothing) used in the proposed algorithm. In Figure 11, we show the comparison of model probability in the IMM algorithm. Model 1 corresponds to the case where the target has a constant velocity and
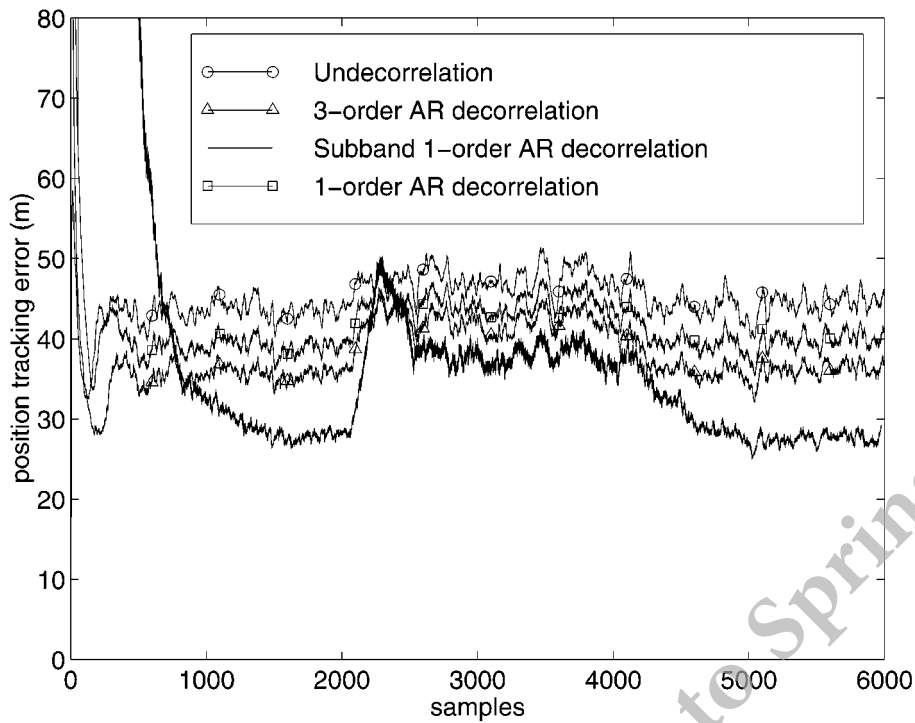
Figure 8. Performance comparison for target position tracking.

model 3 corresponds to the case where the target has a constant acceleration. We can find that the probabilities associated with these two models are not significantly different for the algorithms in Figures 11(a, b, d). In contrast, the proposed algorithm, which is in Figure 11(c), can clearly tell if the target is maneuvering or nonmaneuvering. Apparently, the tracking performance of the proposed algorithm is superior to others.

Although the proposed algorithm performs satisfactorily in the above simulations, the delay is 15. In Figures 12–14, we compare the performance for $l = 15$ and $l = 0$. As we can see, the performance difference between these two cases is not significant, especially when the target is nonmaneuvering. The above simulations are performed with the decorrelation method in (58). Note that the decorrelation method in (58) still requires a delay. Thus, we perform other simulations to test the tracking performance without this delay. The results are also shown in Figures 12–14. In these figures, the biased decorrelation method corresponds to that in (66) without $B(m)$ and the bias-removed decorrelation method corresponds to that in (66) with $B(m)$. It is apparent that the biased decorrelation has poor performance after target maneuvering since the bias is proportional to target velocity. We also can see that the performance difference between the bias-removed decorrelation method and the delayed decorrelation method in (58) is small when the target is nonmaneuvering. That is because in this case the bias is a constant. When target is maneuvering, the difference between two successive position samples is not constant, the bias-removed algorithm is then somewhat degraded. Figure 15 shows no obvious difference in modeling probability for the four simulation cases considered here.
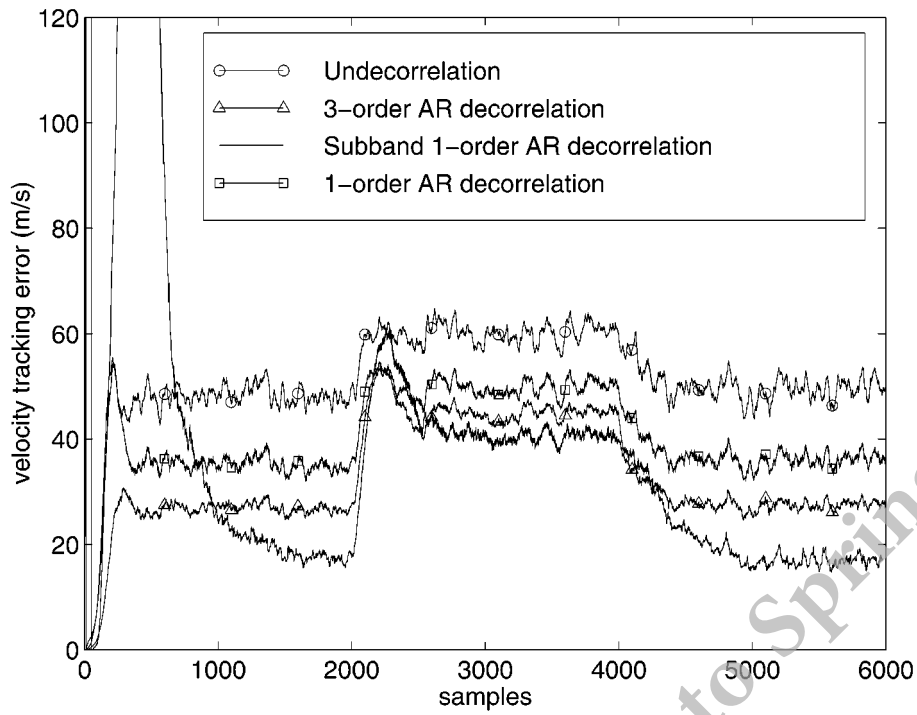
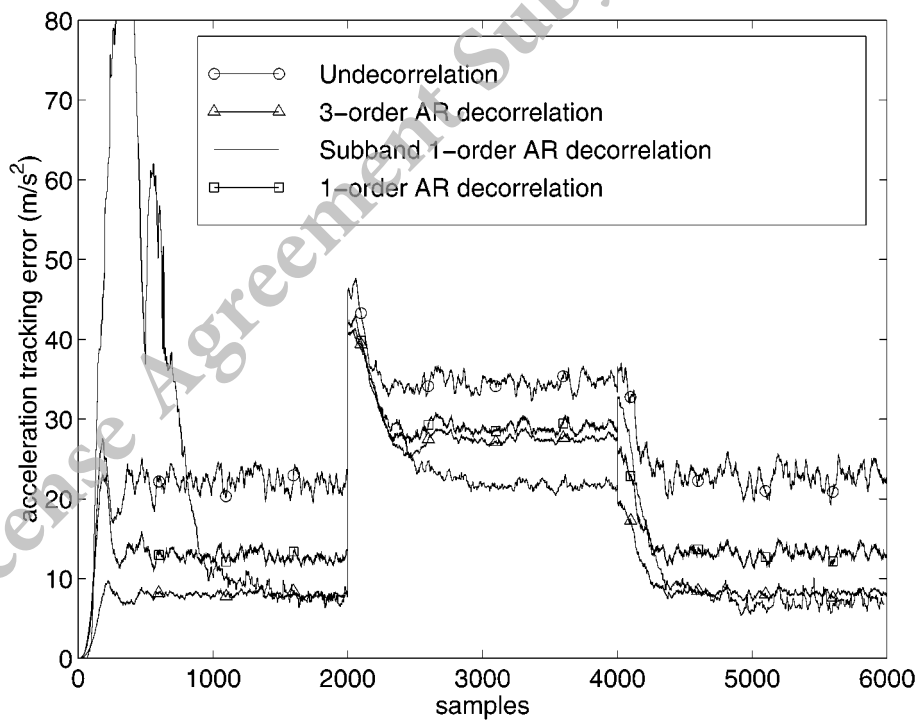*Figure 9.* Performance comparison for target velocity tracking.

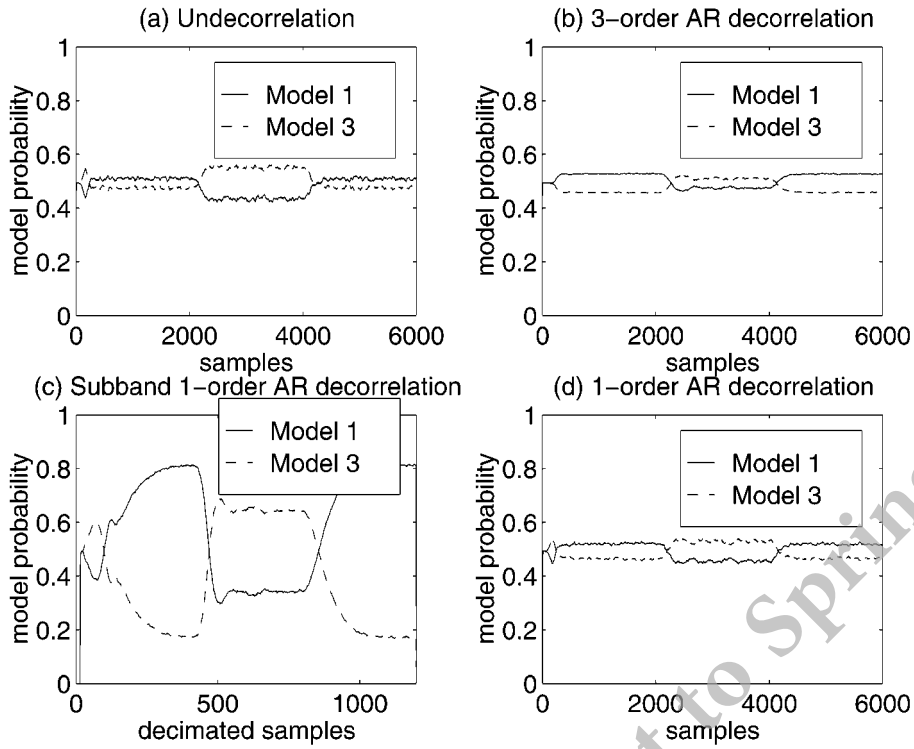*Figure 10.* Performance comparison for target acceleration tracking.

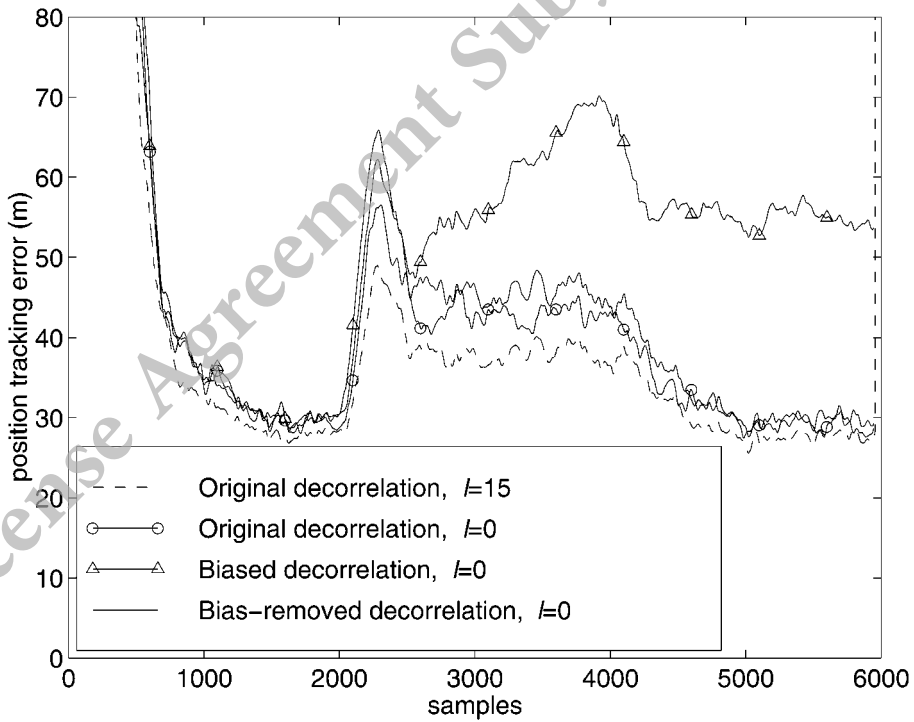*Figure 11.* Comparison of model probability in the IMM algorithm.

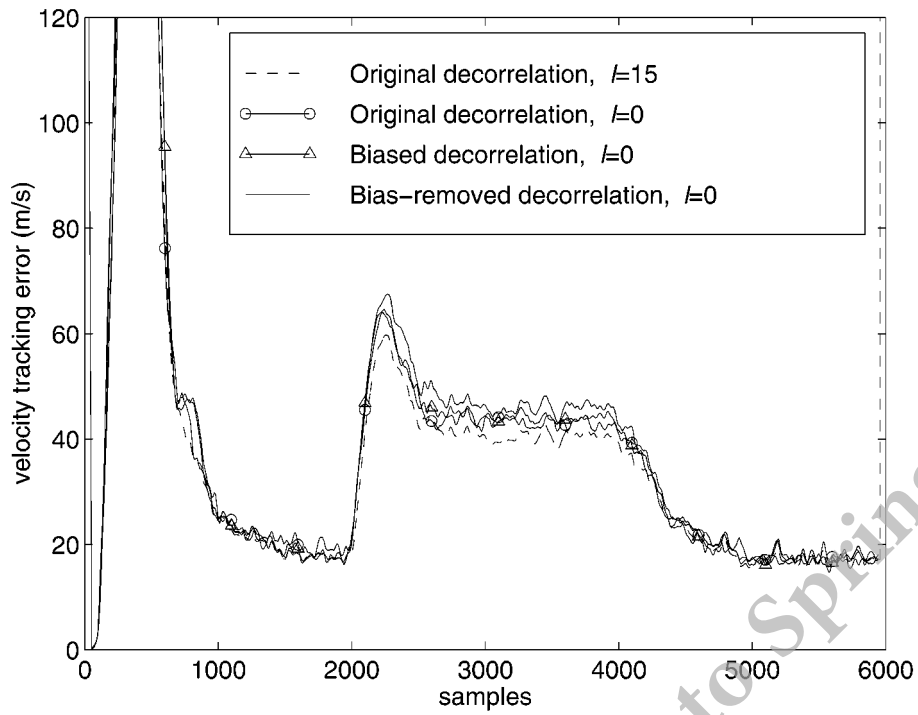*Figure 12.* Performance comparison for target position tracking.

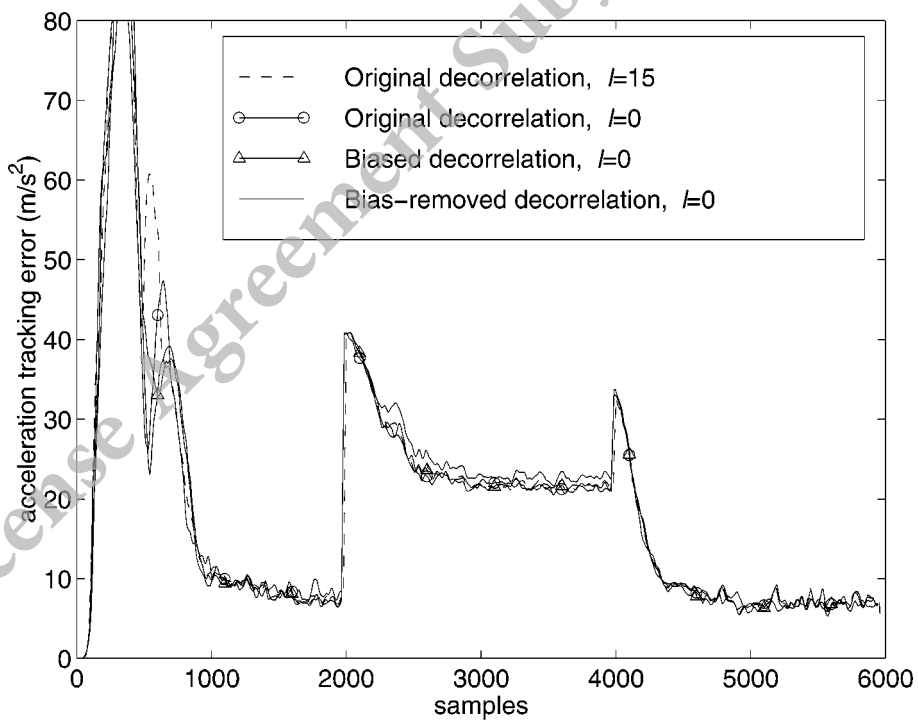*Figure 13.* Performance comparison for target velocity tracking.

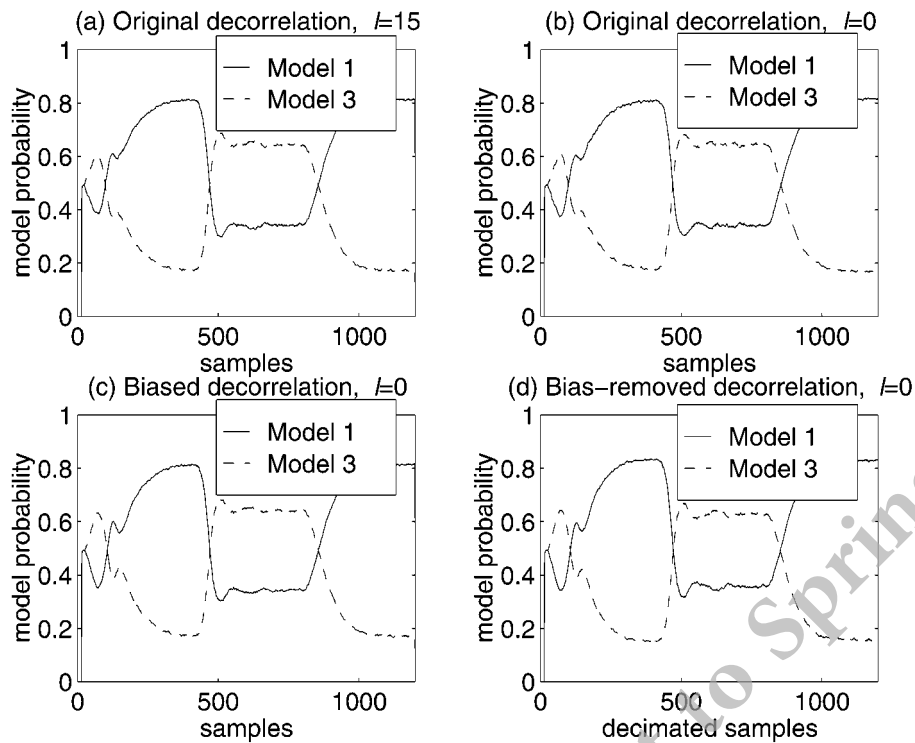*Figure 14.* Performance comparison for target acceleration tracking.

*Figure 15.* Comparison of model probability in the IMM algorithm.

5. Conclusions

We have proposed a new algorithm for maneuvering target tracking with high-order correlated noise. The distinct feature of our approach is that we use the subband processing technique. The measurement signal is first decomposed into subbands and the correlated noise in each band is modeled by a first-order AR process. An online AR identification algorithm is applied to obtain the corresponding AR parameters. A multirate state space model is then built and a newly developed multirate Kalman synthesis filter is used to obtain the state estimate. This algorithm can be incorporated into the IMM algorithm such that the performance can be further enhanced. Simulations show that the proposed algorithm outperforms the existing algorithms.

References

1. W.R. Wu and D.C. Chang, "Maneuvering Target Tracking with Colored Noise", *IEEE Trans. Aerospace and Electronic Systems*, Vol. 32, No. 4, pp. 1311–1320, 1996.
2. S.R. Rogers, "Alpha-Beta Filter with Correlated Measurement Noise", *IEEE Trans. Aerospace and Electronic Systems*, Vol. 23, No. 4, pp. 592-594, 1987.
3. S.R. Rogers, "Continuous-Time ECV and ECA Track Filters with Colored Measurement Noise", *IEEE Trans. Aerospace and Electronic Systems*, Vol. 26, pp. 663–666, 1990.
4. C.C. Arcasoy and B. Koc, "Analytical Solution for Continuous-Time Kalman Tracking Filters with Colored Measurement Noise in Frequency Domain", *IEEE Trans. Aerospace and Electronic Systems*, Vol. 30, pp. 1059-1063, 1994.
5. M. Skolnik, *Radar Handbook*, 2nd edn, McGraw-Hill: New York, 1991.
6. A.E. Bryson and L.J. Henrikson, "Estimation Using Sampled Data Containing Sequentially Correlated Noise", *Journal of Spacecraft*, Vol. 5, No. 6, pp. 662–665, 1968.

7. J.A. Guu and C.H. Wei, "Maneuvering Target Tracking Using IMM Method at High Measurement Frequency", *IEEE Trans. Aerospace and Electronic Systems*, Vol. 27, No. 3, pp. 514–519, 1991.

8. J.A. Guu and C.H. Wei, "Tracking Technique for Maneuvering Target with Correlated Measurement Noise and Unknown Parameters", *IEE Proceedings, Pt. F.*, Vol. 138, No. 3, pp. 278–288, 1991.

9. R. Gazit, "Digital Tracking Filters with High Order Correlated Measurement Noise", *IEEE Trans. Aerospace and Electronic Systems*, Vol. 33, No. 1, pp. 171–177, 1997.

10. L. Hong, "Multiresolutional Filtering Using Wavelet Transform", *IEEE Trans. Aerospace and Electronic Systems* Vol. 29, No. 4, pp. 1244–1251, 1993.

11. L. Hong, "Multiresolutional Distributed Filtering", *IEEE Trans. Automatic Control*, Vol. 39, No. 4, pp. 853–856, 1994.

12. L. Hong, "Multiresolutional Multiple-Model Target Tracking", *IEEE Trans. Aerospace and Electronic Systems*, Vol. 30, No. 2, pp. 518–524, 1994.

13. B.S. Chen, C.W. Lin and Y.L. Chen, "Optimal Signal Reconstruction in Noisy Filter Bank Systems: Multirate Kalman Synthesis Filtering Approach", *IEEE Trans. Signal Processing*, Vol. 43, No. 11, pp. 2496–2504, 1995.

14. Y.L. Chen, K.W. Tay and B.S. Chen, "Model-Based Filter Banks and Corresponding Subband Coding Systems: Multirate State-Space Approach", *Signal Processing*, Vol. 55, pp. 257–268, 1996.

15. Y. Bar-Shalom and T.E. Fortman, *Tracking and Data Association*, Academic Press: New York, 1988.

16. G.A. Hewer, R.D. Martin and J. Zeh, "Robust Preprocessing for Kalman Filtering of Glint Noise", *IEEE Trans. Aerospace and Electronic Systems*, Vol. 23, No. 1, pp. 120–128, 1987.

17. T.C. Wang and P.K. Varshney, "Measurement Preprocessing Approach for Target Tracking in a Cluttered Environment", *IEE Proceedings-F, Radar, Sonar and Navigation*, Vol. 141, No. 3, pp. 151–158, 1994.

18. W.R. Wu and D.C. Chang, "Target Tracking by Using the Median Filter as a Preprocessor", *The 7th International Conference on Signal Processing Applications and Technology*, Boston, MA, Oct. 7–10, 1996, pp. 1469–1473.

19. D.C. Chang and W.R. Wu, "A Feedback Median Filter for Robust Preprocessing of Glint Noise", *IEEE Trans. Aerospace and Electronic Systems*, Vol. 36, No. 4, pp. 1026–1035, 2000.

20. Y. Bar-Shalom, K.C. Chang and H.A.P. Blom, "Tracking a Maneuvering Target Using Input Estimation versus the Interacting Multiple Model Algorithm", *IEEE Trans. Aerospace and Electronic Systems*, Vol. 25, No. 3, pp. 296–300, 1989.

21. J.P. Princen and A.B. Bradley, "Analysis/Synthesis Filter Bank Design Based on Time Domain Aliasing Cancellation", *IEEE Transactions on Acoustics, Speech, Signal Processing*, Vol. 34, No. 5, pp. 1153–1161, 1986.

22. M. Vetterli and C. Herley, "Wavelets and Filter Banks: Theory and Design", *IEEE Transactions on Signal Processing*, Vol. 40, No. 9, pp. 2207–2232, 1992.

23. T.Q. Nguyen and P.P. Vaidyanathan, "Structures for M-Channel Perfect-Reconstruction FIR QMF Banks Which Yield Linear-Phase Analysis Filters", *IEEE Transactions on Acoustics, Speech, Signal Processing*, Vol. 38, No. 3, pp. 433–446, 1990.

24. K. Nayebi, T.P. Barnwell, III and M.J.T. Smith, "Time-Domain Filter Bank Analysis: A New Design Theory", *IEEE Transactions on Signal Processing*, Vol. 40, No. 6, pp. 1412–1428, 1992.
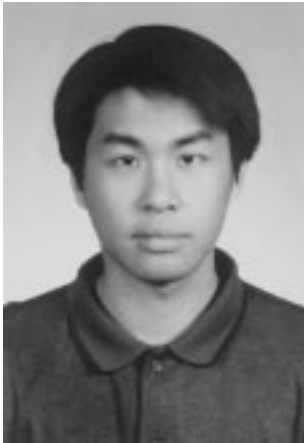
Dah-Chung Chang was born in Chia-Yi, Taiwan, on 13 June 1969. He received his B.S. degree in electronic engineering from the Fu-Jen Catholic University, Taipei, in 1991 and his M.S. and Ph.D. degrees in electrical engineering from the National Chiao Tung University, Hsinchu, in 1993 and 1998, respectively.

In 1998, he joined Computer and Communications Research Laboratories at Industrial Technology Research Institute, Hsinchu, where he is currently working on system simulation and circuit design for broadband communication systems. His research interests include multirate digital signal processing, detection and estimation theory, VLSI architecture and their applications to multimedia signal processing, digital communications, radar tracking, and biomedical engineering.

Wen-Rong Wu was born in Taiwan in 1958. He received his B.S. degree in mechanical engineering from Tatung Institute of Technology, Taiwan, in 1980 and his M.S. degrees in mechanical and electrical engineering and Ph.D. degree in electrical engineering from the State University of New York at Buffalo in 1985, 1986, and 1989, respectively.

Since August 1898, he has been a faculty member of the Department of Communication Engineering at the National Chiao Tung University, Taiwan. His research interests include statistical signal processing and digital communications.